This project has received funding from the European Union's Seventh Framework Programme for research, technological development and demonstration under grant agreement no. 289437

ARANGE Deliverable D1.4

Climate Change Scenarios for Case Study Regions

09.07.2013

Heimo Truhetz

Document Properties

Document number	FP7-289437-ARANGE / D1.4
Document title	D1.4 Climate Change Scenarios for Case Studies
Author(s)	Heimo Truhetz
Date of last revision	05.09.2013
Status	draft
Version	1.0
Dissemination level	PU
Relation	WP 1 (T1.2), related to T1.2, WP 2, WP 5

The research leading to these results has received funding from the European Community's Seventh Framework Programme (FP7/2007-2013) under grant agreement n° 289437.

Keywords:

Climate change scenarios, multi-model ensemble, uncertainty, bias correction, ENSEMBLES

Abstract:

Deliverable D1.4 makes climate change and its uncertainty accessible to ARANGE. Based on the ensemble of regional climate simulations from the EU FP6 project ENSEMBLE a set of five transient simulations (representing uncertainty) is statistically downscaled to each of the seven ARANGE case study regions by means of quantile mapping. Each of the downscaled climate change scenarios is represented by time series of 100 years (2001 to 2100) on daily basis for temperature, precipitation, water vapor deficit, and solar radiation.

TABLE OF CONTENTS

1 Introduction

One of the aims of the EU-FP7 project ARANGE (www.arange-project.eu) is to assess climate change effects on ecosystem service (ES) provisioning in mountainous regions in Europe. In order to analyze conflicts and complementarities among ES from stand to landscape scales, improved models for the assessment and projection of ES as well as novel planning and decision support tools are developed and applied in seven case study regions. The methodological approach grounds on state-of-the-art models for forest dynamics and ES assessment, which are driven by meteorological data representing current and possible future climate conditions.

The objective of task T1.2 in work package WP 1 is to make climate change and its uncertainty accessible to the project. For all case study regions, transient climate change scenarios covering a planning period up to the year 2100 are provided based on selected regional climate simulations from the EU FP6 project ENSEMBLES (Hewitt and Griggs, 2004; www.ensembles-eu.org). The wide range of regional climate simulations from ENSEMBLES enables to assess uncertainty in climate change projections and forms the basis for a skillful selection of a subset of five representative climate scenarios, which reasonably span the range of uncertainty. These representative scenarios are post-processed with empirical-statistical techniques in order to reduce biases and to adapt the climate scenarios to the specific local climate conditions of the case study regions as represented by the baseline climate (see Deliverable D1.1, and Thurnher 2013). Finally, transient time series until the end of the 21st century on a daily basis are derived from the five representative scenarios and handed over to the consortium.

2 Available Datasets

During the ENSEMBLES project, 22 (15) highly resolved (~25 km grid spacing) regional climate model (RCM) simulations until the middle (end) of the 21st century have been conducted for the European continent. The simulations were driven by eight different global climate models (GCMs) employing the greenhouse gas (GHG) emission scenario A1B (Nakicenovic et al., 2000). Due to limited computational resources, not all possible GCM/RCM combinations could be realized (cf. Table 1), but the simulation matrix is still dense enough to cover uncertainty in climate change to a reasonable extend (van der Linden and Mitchell, 2009; Heinrich et al., 2013).

For ARANGE, only those simulations reaching the end of the 21st century are of interest. This reduces the number of simulations to 15. Since there is some concern about the physical consistency of one of the ENSEMBLES simulations (Wilcke et al., 2013), the number of simulations is further reduced. In total, 14 simulations are qualified for task T1.2 (cf. Table 1).

Each of the 14 simulations consists of 2D fields (~25 km grid spacing) on a daily basis (i.e. time series of daily values from the 2nd half of the 20th century to the end of the 21st century) for the variables maximum temperature, minimum temperature, precipitation, and global radiation.

Table 1: GCM/RCM matrix of the ENSEMBLES project. 22 climate simulations reaching the middle of the 21st century are marked by grey areas, the orange areas indicate 15 simulations reaching the end of the 21st century. Simulations used in ARANGE are marked with "X" in yellow cells.

		8 Global Climate Models (GCMs)							
		ARPEGE	BCM	CGCM3	ECHAM5-r3	HadCM3Q0	HadCM3Q3	HadCM3Q16	IPSL
15 Regional Climate Models (RCMs)	C4I_RCA								
	CNRM_ALADIN4.5								
	CNRM_ALADIN5.1	X							
	DMI_HIRHAM	X	X		X				
	ETHZ_CLM					X			
	GKSS_CLM								
	ICTP_RegCM				X				
	KNMI_RACMO				X				
	METNO_HIRHAM								
	HC_HadCM3					X	X	X	
	MPI_REMO				X				
	OURANOS_CRCM								
	SMHI_RCA		X		X		X		
	UCLM_PROMES								
	VMGO_RRCM								

The second input data represents local conditions of the current climate (the baseline climate) in each of the study regions provided by task T1.2 (Thurnher 2013; D1.1). The baseline climate consists of stochastic time series data on daily basis (maximum temperature, minimum temperature, daylight temperature, precipitation, global radiation, and vapor pressure deficit). These time series were generated by the weather generator LARS-WG (Racsko et al., 1991; Semenov and Barrow, 1997) on the grounds of observational data and post-processed with MT-CLIM (Running et al., 1987; Thornton and Running, 1999) to implement altitudinal zones, slopes and aspects for a selected number of representative sites in each case study area (CSA). The baseline climate is derived from station data and E-OBS (Haylock et al., 2008) from the period 1961 to 1990. Though generated by a weather generator, the baseline climate reflects the statistical properties of the climate during the reference period.

3 Methodological Approach

In order to derive climate change scenario data (i.e. the driving data for the forest and ES models) in each case study region from the two sources of input data, the ENSEMBLES climate simulations and the baseline climate, three steps have to be accomplished:

(1) The climate simulations need to be downscaled to the case study regions and corrected for biases.

(2) Since the climate simulations do not contain daylight temperature and vapour pressure deficit, these variables need to be derived from available data.

(3) Five climate simulations have to be selected in a way, so that the full range of the ENSEMBLES simulations is covered.

In the following subsections, these three steps are described in detail.

3.1 Downscaling and Bias Correction

The ENSEMBLES simulations are given on a grid with ~25 km grid spacing while the baseline climate (treated as point-wise data) is representative for each case study region and is given for different altitudes, slopes and aspects. In order to accomplish (1) bridging the gap in scales, (2) taking account for local orographic effects, and (3) correcting the error characteristics of the simulations, a quantile based approach (Quantile Mapping; QM; Dobler and Ahrens, 2008; Piani et al., 2010; Themeßl et al., 2011) is applied.

QM originates from the empirical transformation of Panofsky and Brier (1968) and can be classified as a distribution based model output statistics approach (Maraun et al., 2010). It is an empirical-statistical downscaling and error correction method (DECMs) that aims at adjusting the empirical cumulative distribution functions (ECDFs) of model data towards a reference data (cf. Figure 1) and therefore accounts for errors in the shape of the modelled distribution (Themeßl et al., 2011; Déqué, 2007). The potential of QM for correcting GCM data has been demonstrated by e.g. Dettinger et al. (2004) and Wood et al. (2004). In ARANGE, QM has been selected to be applied on RCM data as it already has proofed its robustness and superior performance even for non-normally distributed parameters such as daily precipitation (e.g. Dobler and Ahrens, 2008; Themeßl et al., 2011; 2012; Piani et al., 2009; Finger et al., 2012). Nonetheless, one has to bear in mind that QM affects the climate change signal and relies on the assumption, that the relationship between statistical properties of the model output of the control simulation and the observational data is not affected by climate change. In other words, this relationship is supposed to be stationary. However, even in the worst cases of non-stationarity, QM still clearly improves biases of the raw RCM output (Wilcke et al., 2013).

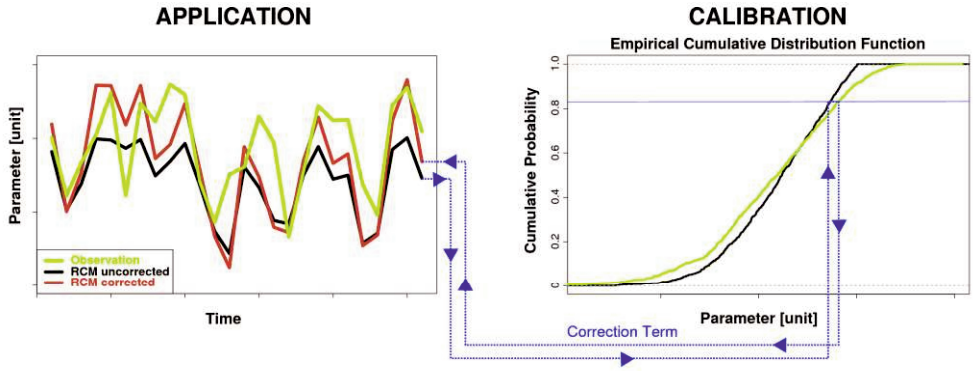

Figure 1: Generation of error corrected time series by mapping the uncorrected RCM values (black) to reference data from the calibration period (green).

The application of QM within ARANGE builds up on point-wise (the case study regions are independent from each other) and daily time series. A 31-day moving window covering all years in the training period (1961 to 1990) centred on the day to be corrected is used for constructing this particular day of the year. This enables annual-cycle sensitive correction as well as a sufficiently large sample size. The baseline climate (used as reference data) is given for each case study region which is associated with its central point. The surrounding four grid cells in the raw RCM data are linearly interpolated to the central point of the study region giving the climate simulation data to be corrected. Due to the linear interpolation, influences from multiple grid cells are taken into account which increases the reliability of the method. Variables of concern are: maximum temperature, minimum temperature, precipitation, and global radiation.

Since the baseline climate takes account of local effects in each case study region and since the baseline climate is used to calibrate the QM method, the local effects are persevered in the corrected RCMs' output. However, this is only valid within the limits of the method, i.e. as long as the principle of stationarity is not affected by climate change.

QM is generally applicable to any of the meteorological variables, however some specific details have to be regarded, especially for precipitation. Dealing with precipitation, a frequency adaptation is implemented to parry a deficiency of QM leading to a wet bias. That bias occurs if the dry day frequency in the raw RCM is larger than in the reference data. The overestimation would lead to a positive bias after the correction step (Themeßl et al., 2012). Although this bias is a rare case and the RCM overestimates light precipitation frequency ("drizzling-effect"; e.g. Gutowski et al., 2003) more often, it can regionally result in considerable biases. Therefore, the model data below 0.1 mm is divided to finer bins with width of 0.01 mm. Dry days are generated by randomly sampling the observational distribution into the first bin (0.00 mm - 0.01 mm). This completely removes the artificially introduced bias.

3.2 Calculation of Missing Variables

Not all ENSEMBLES simulations contain the year 2100 completely. In such cases, the last complete year (i.e. 2098) is repeated in order to generate time series reaching December 31st, 2100.

The ENSEMBLES simulations do not contain all requested variables. For instance, daylight temperature and vapour pressure deficit are missing. These variables are calculated from downscaled and corrected variables. Thereby, the same empirical relations are applied as they have been used in calculating the baseline climate: daylight temperature is calculated from maximum and minimum temperature, vapour pressure deficit is calculated from daylight temperature and minimum temperature (cf. Thurnher, 2013):

Equation 1 $tday = 0.45 * (tmax - tavg)$, with $tavg = (tmax + tmin)/2$

tday ... daylight temperature [°C]
tmax ... maximum temperature [°C]
tmin ... minimum temperature [°C]

Equation 2 vpd = 610.7 * [exp((17.38 * tday)/(tday + 239)) - exp((17.38 * tmin)/(tmin + 239))]

vpd ... vapour pressure deficit [Pa]

The ENSEMBLES models do not have the same calendar. Some models use the Julian, some the Gregorian calendar, some have a fixed calendar with 360 days per year. Since the baseline climate has a time axis with 365 days per year (cf. Thurnher, 2013), the ENSEMBLES simulations have to be converted to this scheme. This is accomplished in the following way: If the simulation has the Gregorian calendar, the 29th Februarys of the leap years are simply skipped. In the case of a 360 day calendar, the missing five days (May 31st, July 31st, August 31st, October 31st, December 31st) are linearly interpolated from their surrounding days as this approach has proven successful in other climate change impact studies (e.g. CLAVIER, ACQWA, IMPACT2C).

3.3 Selection of Climate Change Scenarios

In climate projections, uncertainty is determined by three components:

(1) Natural variability

This component includes variations that are directly driven by periodic external forcings (e.g. the seasonal cycle), variations due to the non-linear interplay of feedbacks within the climate system (e.g. ice-albedo feedback), and variations associated with random fluctuations in physical (e.g. weather) or chemical factors (Ghil, 2002).

(2) External forcings

These refer to anthropogenic forcing due to the emission of greenhouse gases and land use changes.

(3) Model formulation

Climate models represent simplified (imperfect) approximations to an incompletely understood climate system (Stainforth et al., 2007).

Uncertainty due to natural variability in the ENSEMBLES simulations was implicitly regarded via the use of different GCMs, but uncertainty due to the GHG emission scenario was not included (all simulations where driven by one GHG scenario). A rough estimate to which extend the overall uncertainty is underestimated by only using one emission scenario can be obtained from Prein et al. (2011). The authors analyzed temperature and precipitation over Europe of 84 simulations from 23 GCMs and found: the relative contribution of the emission scenario to uncertainty until mid of the 21st century is very small (below 6 %) for both variables; by end of the century, this fraction increases regarding to temperature up to 35 %, but remains very small with regard to precipitation; the largest source of uncertainty is the formulation of the climate models themselves. In addition, RCMs are also known to feature substantial model errors (e.g. Frei et al., 2003; Hagemann et al., 2004; Suklitsch et al., 2008, 2011) which affect the assessment of climate change impacts. This strongly pronounces the large influence of climate models and hence the selection of climate simulations is not straightforward. One of the open questions is whether models should be weighted with respect to their performance for representing current climate conditions. However, there is no consensus in the current discussion about suitable

performance metrics (Tebaldi and Knutti, 2007) and weighted model ensembles have not clearly demonstrated their advantages over un-weighted ensembles (e.g., Knutti et al., 2010; Déqué and Somot, 2010).

Due to the importance of the models and the inconclusive discussion on model weighting, the selection of the subset of five representative simulations is purely based on the spread of the ENSEMBLSE simulations. Nevertheless, since knowledge about the climate system is incomplete and climate models are simplified pictures of the known part of the climate system, there is an inherent chance for underestimating uncertainty. Hence, estimating uncertainty by means of a limited number of (imperfect) simulations is the working hypotheses in task T1.2.

The selection process is based on error corrected mean daily daylight temperature and mean daily precipitation changes of the summer half year, since these variables are supposed to have most impact on forest and ES models (Lexer M., personnel communication). In the case there is large precipitation (e.g. in case study region 5, the Scandinavian mountains) global radiation is also taken into account. This reduces the number of investigated variables to a maintainable size. In order to mimic the ENSEMBLES range, those four simulations outlining the ENSEMBLES range and one lying next to the ensembles median are selected. Thereby, the two 30 year periods 1961 to 1990 and 2071 to 2100 are used to calculate mean climate change signals of concern.

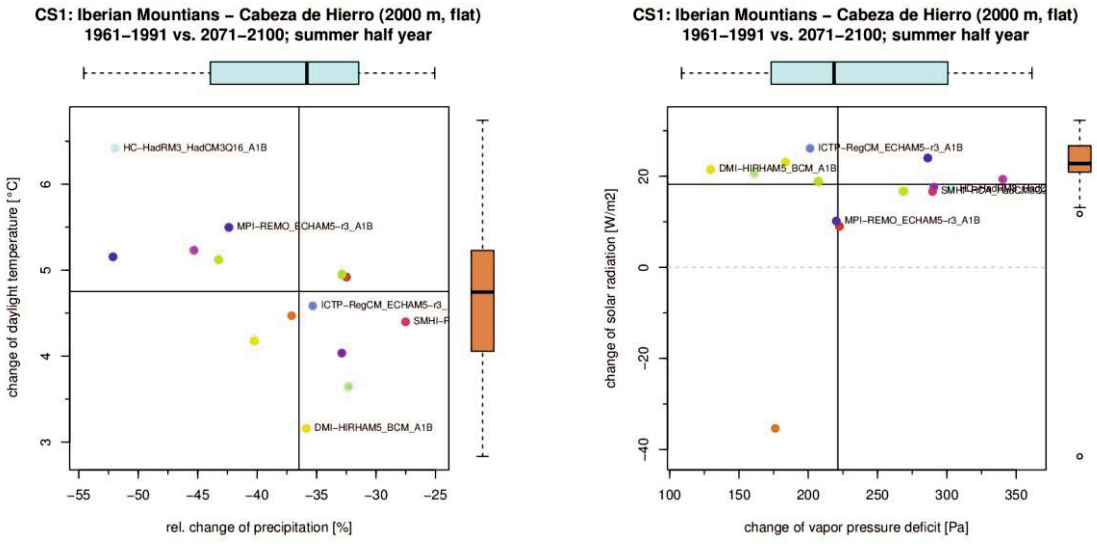

Figure 2: Climate change signals of daylight temperature [°C], precipitation [%], solar radiation [W/m^2], and vapor pressure deficit [Pa] in case study region CS1, Cabeza de Hierro, on a flat plane elevated to 2000 m. Differences between the periods 1961 to 1990 and 2071 to 2100 of the half year means (April 16th to September 15th) from downscaled and corrected ENSEMBLES simulations are shown. Selected representative simulations are labeled.

This selection process is conducted separately for each case study region. Table 2 lists the selected simulations per case study region.

Table 2: Selected simulations for the case study regions rendering climate change uncertainty.

Case study	Member of the ENSEMBLES ensemble				
CS1	HC-HadRM3_HadCM3Q16	DMI-HIRHAM5_BCM	ICTP-RegCM_ECHAM5-r3	SMHI-RCA_HadCM3Q3	MPI-REMO_ECHAM5-r3
CS2	HC-HadRM3_HadCM3Q16	DMI-HIRHAM5_BCM	HC-HadRM3_HadCM3Q3	SMHI-RCA_HadCM3Q3	MPI-REMO_ECHAM5-r3
CS3	HC-HadRM3_HadCM3Q16	DMI-HIRHAM5_BCM	HC-HadRM3_HadCM3Q3	HC-HadRM3_HadCM3Q0	SMHI-RCA_HadCM3Q3
CS4	HC-HadRM3_HadCM3Q16	DMI-HIRHAM5_BCM	SMHI-RCA_HadCM3Q3	DMI-HIRHAM5_ARPEGE	SMHI-RCA_HadCM3Q3
CS5	HC-HadRM3_HadCM3Q16	DMI-HIRHAM5_BCM	DMI-HIRHAM5_ARPEGE	KNMI-RACMO2_ECHAM5-r3	MPI-REMO_ECHAM5-r3
CS6	HC-HadRM3_HadCM3Q16	DMI-HIRHAM5_BCM	DMI-HIRHAM5_ARPEGE	ICTP-RegCM_ECHAM5-r3	SMHI-RCA_ECHAM5-r3
CS7	HC-HadRM3_HadCM3Q16	DMI-HIRHAM5_BCM	DMI-HIRHAM5_ARPEGE	KNMI-RACMO2_ECHAM5-r3	ETHZ-CLM_HadCM3Q0

4 Results

4.1 Evaluation

QM is a well-established technique which already has been successfully employed in numerous climate change impact studies, for instance in the EU funded projects CLAVIER (www.clavier-eu.org), ACQWA (www.acqwa.ch), and IMPACT2C. Evaluation results (partly supported by these projects) have been published by Themeßl et al. (2011; 2012), Finger et al. (2012), and Mendlik et al. (2012). Summing up, QM is a robust and flexible method. It successfully draws erroneous frequency distributions from climate models towards those of the reference data and corrects biases by at least one magnitude. Latest investigations have shown, that QM affects the physical consistency (given by the climate model) between multiple meteorological variables, correlation coefficients, and auto correlation in a negligible way (Wilcke et al., 2013) as long as climate change signals for averaged quantities (e.g. mean values) are investigated.

In ARANGE, the reference data is given by the baseline climate which is generated by a weather generator (based on observational data) and modified by empirical relationships in order to capture local effects of altitude, slopes and aspects. Although given in time series on a daily basis, the baseline climate does not exactly match the time series of historical weather conditions. It does also not show any historical trend, however other statistical properties (e.g. frequency distributions, mean values) of the underlying observational data are well captured (Thurnher, 2013). Hence, this subsection focuses on demonstrating the effect of QM as it is employed in ARANGE.

In case study region CS1, the simulation MPI-REMO_ECHAM5-r3 is one of the representative climate simulations (cf. Figure 2 and Table 2). Looking at monthly mean biases of the simulation with respect to the reference period (1961 to 1990), one may easily see that MPI-REMO_ECHAM5-r3 overestimates (underestimates) daily maximum temperatures (daily minimum temperatures) by 0.6°C (-1.5°C) on average (cf. Figure 3) and shows monthly biases in the range from -0.3°C (-2.5°C) and 1.7°C (-0.6°C). When QM is applied, the biases are corrected: the overall bias nearly disappears and the mean monthly biases vary between -0.2°C (-0.1°C) and 0.3°C (0.3°C) (cf. Figure 3). This fundamental behaviour of bias reduction is observed for the other variables, too (cf. Figure 4 and Figure 5), and it is also observed for the derived variables (daylight temperature and vapour pressure deficit, cf. Figure 5): since MPI-REMO_ECHAM5-r3 underestimates minimum temperature, but captures daylight temperature quite well, vapour pressure deficit is overestimated by 93.3 Pa on the annual mean (200 Pa in the August average; cf. Figure 5) following the dependency of vapour pressure deficit from daylight and minimum temperature (cf. Equation 2). Deriving vapour pressure deficit from corrected temperatures also leads to a correction in the derived variable: the annual bias is reduced to -3.2 Pa and the monthly biases range between -18.2 Pa and 14.6 Pa. The strengths of QM become most apparent for global radiation: in this specific case, a big underestimation of solar radiation (-166.6 W/m^2 on the annual mean) is drastically reduced (to -1.1 W/m^2 as annual mean value) and the seasonality of the biases is largely corrected (cf. Figure 4).

However, the inter annual spread of biases (expressed in terms of whiskers in Figure 3, Figure 4, and Figure 5) remains. This is related to the limits of the correction method: since QM does not affect the correlation coefficient, a reduction of the spread cannot be expected.

This systematic correction of RCM biases due to the application of QM has been found for all simulations and in all case study regions.

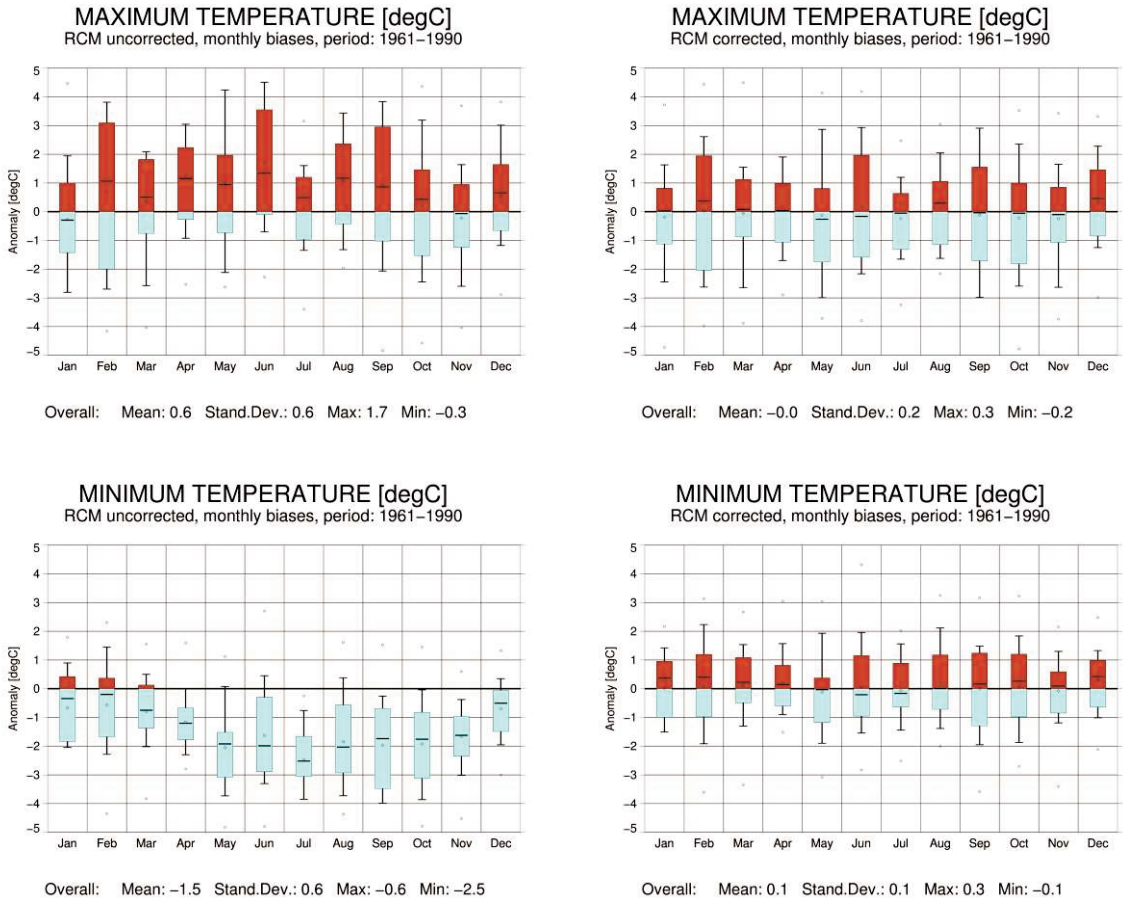

Figure 3: Monthly biases for daily maximum and minimum temperature of the simulation MPI-REMO_ECHAM5-r3 (left column: raw model output; right column: after bias correction) of the period 1961 to 1990 in case study region CS1, Cabeza de Hierro, on a flat plane elevated to 2000 m.

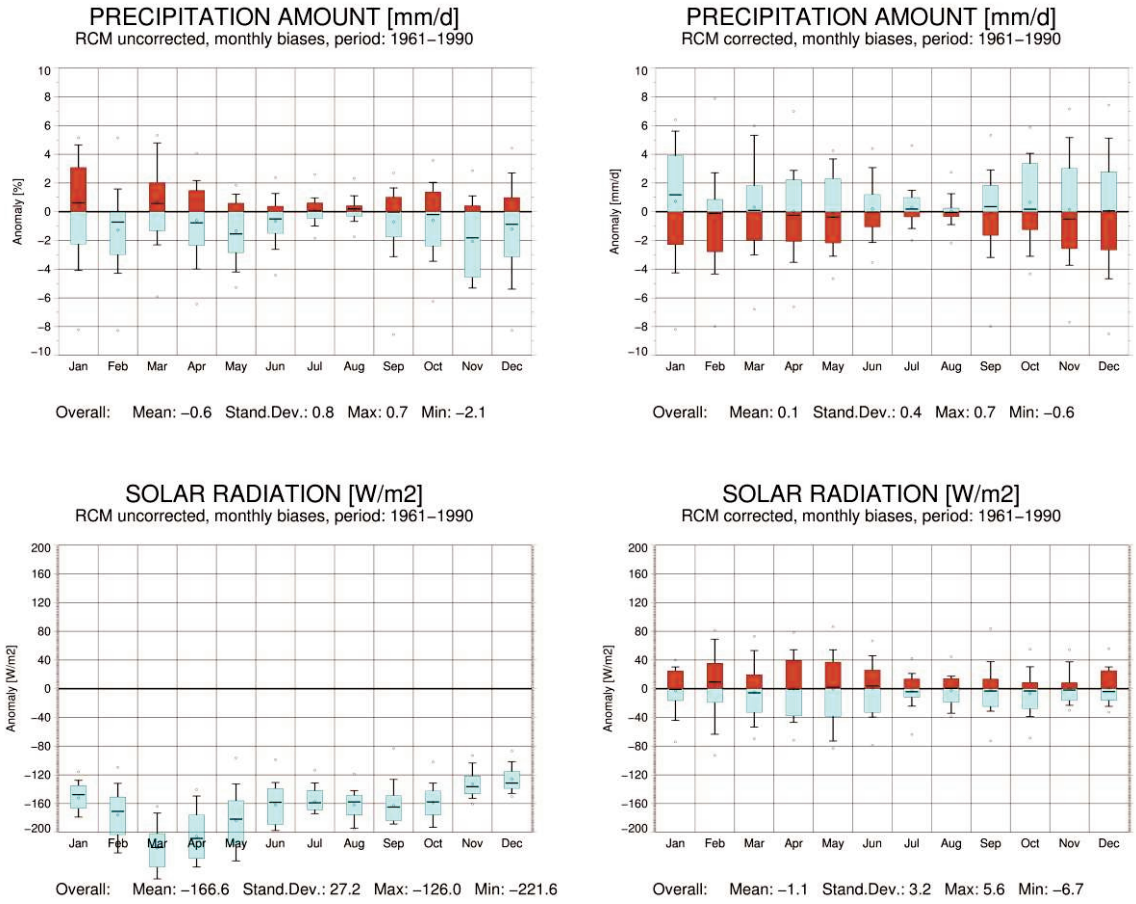

Figure 4: Same as Figure 3, but for precipitation and solar radiation.

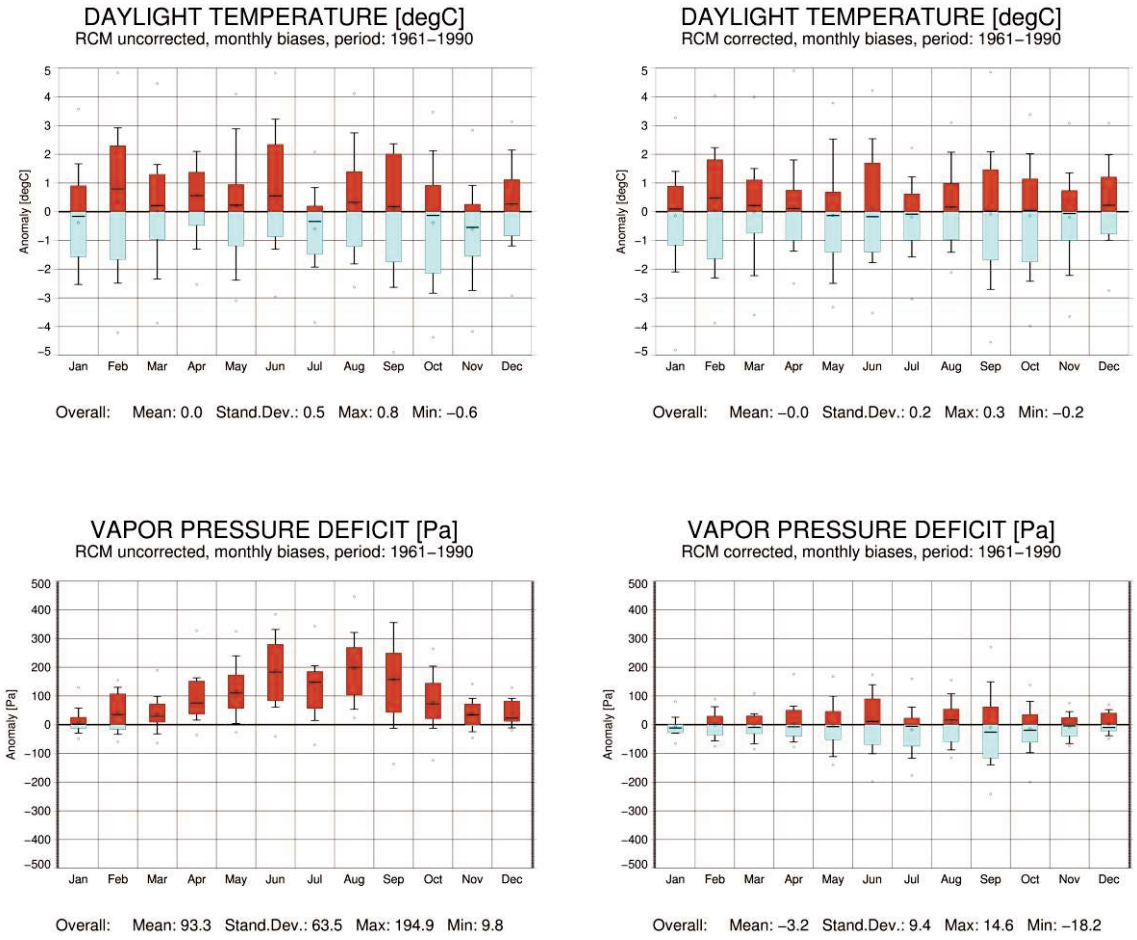

Figure 5: Same as Figure 3, but for the derived variables daylight temperature and vapour pressure deficit.

4.2 Representative Climate Change Scenarios

An overview of climate change effects on all variables in all case study regions is shown in Table 3. While temperatures and temperature based variables (like vapour pressure deficit) are expected to increase throughout the case study regions, precipitation and solar radiation do not show such a consistent behaviour. In addition to regional deviations (increase in Northern Europe, decrease in Southern Europe; also known as the European Climate Change Oscillation (Giorgi and Coppola, 2007; Heinrich et al., 2013)), precipitation also shows deviations along the annual cycle (shifts to positive changes in the winter half year). For instance, in CS4, the Dinaric Mountains, precipitation is expected to decrease in summer and to increase in winter. In CS3, the Eastern Alps, and CS6, the Carpathians, both options (increase and decrease) seem to be equally possible for precipitation in one half year (i.e. in summer); that means, the five underlying climate simulations partly show a decrease and partly an increase. This indicates high uncertainty in the climate change effect with respect to summer precipitation in that region. Highest uncertainty, in general, may be expected for solar radiation: five out of the seven case study regions experience both, increase as well as decrease.

Table 3: Ranges of climate change signals (2071 to 2100 vs. 1961 to 1990) in the case study regions for a flat plane on highest elevations. Changes of the averaged summer half year (April 16th to September 15th) and winter half year (in parentheses) are shown.

	Daylight temperature [°C]	Maximum temperature [°C]	Minimum temperature [°C]	Precipitation [%]	Water vapour pressure deficit [%]	Solar radiation [%]
CS1 Cabeza (2000 m)	3.2 to 6.4 (3.2 to 5.2)	3.3 to 6.6 (3.5 to 5.6)	2.8 to 5.9 (2.4 to 4.3)	-52.0 to -27.5 (-24.4 to 3.0)	22.7 to 53.3 (55.5 to 85.0)	2.5 to 6.4 (2.2 to 9.6)
CS1 Valsain (2000 m)	3.5 to 6.9 (3.5 to 5.8)	3.5 to 6.9 (3.8 to 6.1)	3.4 to 6.9 (2.7 to 5.1)	-51.9 to -23.6 (-20.6 to 2.4)	21.6 to 52.1 (52.2 to 84.5)	2.5 to 7.8 (2.4 to 10.7)
CS2 (1800 m)	1.7 to 5.3 (3.4 to 5.6)	1.7 to 5.7 (3.6 to 6.0)	1.7 to 4.4 (2.9 to 4.8)	-49.2 to 0.6 (3.8 to 22.8)	10.4 to 52.3 (33.6 to 64.7)	0.1 to 8.4 (-3.9 to 5.2)
CS3 (2000 m)	1.7 to 5.3 (4.0 to 7.4)	1.7 to 5.8 (4.4 to 8.2)	1.7 to 4.1 (3.0 to 5.2)	-26.8 to 13.3 (5.4 to 37.6)	11.1 to 67.0 (65.4 to 151.5)	-2.7 to 7.3 (-6.1 to 2.0)
CS4 (1800 m)	1.4 to 5.0 (2.8 to 6.1)	1.4 to 5.2 (2.8 to 6.5)	1.4 to 4.5 (2.7 to 5.1)	-42.4 to -5.0 (-2.0 to 19.4)	9.4 to 41.9 (25.7 to 70.0)	-12.7 to 3.9 (-7.5 to 3.7)
CS5 (800 m)	2.1 to 5.4 (4.4 to 6.4)	2.1 to 5.7 (4.0 to 6.1)	2.1 to 4.7 (5.3 to 7.2)	2.6 to 28.0 (22.7 to 64.8)	9.4 to 50.3 (24.8 to 56.5)	-11.4 to -0.2 (-6.2 to 1.3)
CS6 (1550 m)	1.2 to 4.5 (3.0 to 6.3)	1.2 to 4.8 (3.1 to 6.6)	1.2 to 3.7 (3.0 to 5.4)	-28.5 to 9.6 (12.3 to 53.8)	7.3 to 43.6 (33.9 to 87.9)	-8.4 to 4.5 (-9.4 to 1.1)
CS7 (2000 m)	2.1 to 6.4 (3.0 to 6.7)	2.2 to 6.8 (3.1 to 7.2)	1.7 to 5.3 (2.7 to 5.3)	-47.9 to -15.8 (-22.3 to -1.9)	18.8 to 65.0 (33.1 to 96.6)	-17.9 to 6.6 (-13.3 to 9.4)

The temporal evolution of temperature, precipitation, vapour pressure deficit, and solar radiation is exemplarily shown for CS1 (Figure 6). These time series of annual mean values depict the climate change effect and its uncertainty in this case study region. From Figure 6 one may see the following effects: (1) the range of the climate simulations increases with time and hence, uncertainty in climate projections for the end of the 21st century is larger than for near future projections. (2) The annual variability of single simulations increases with time and, in particular, becomes larger than the variability of the baseline climate. Hence, changes in meteorological conditions from one year to the next are expected to progressively increase and exceed current conditions.

A complete set of half year changes for all case study regions can be found in the Appendix.

The five selected, downscaled, and corrected climate simulations consist of time series on a daily bases for daylight, minimum, and maximum temperature, precipitation, vapour pressure deficit, and global radiation covering the period 2001 to 2100. They also take account for local characteristics of the orography (altitude, slope and aspect). In the final step these time series are converted into the same file format (Thurnher, 2013) as it is used for the baseline climate. This simplifies the usage of the data in forest and ES models.

The climate change data files are available via the ARANGE Internal Communication Platform.

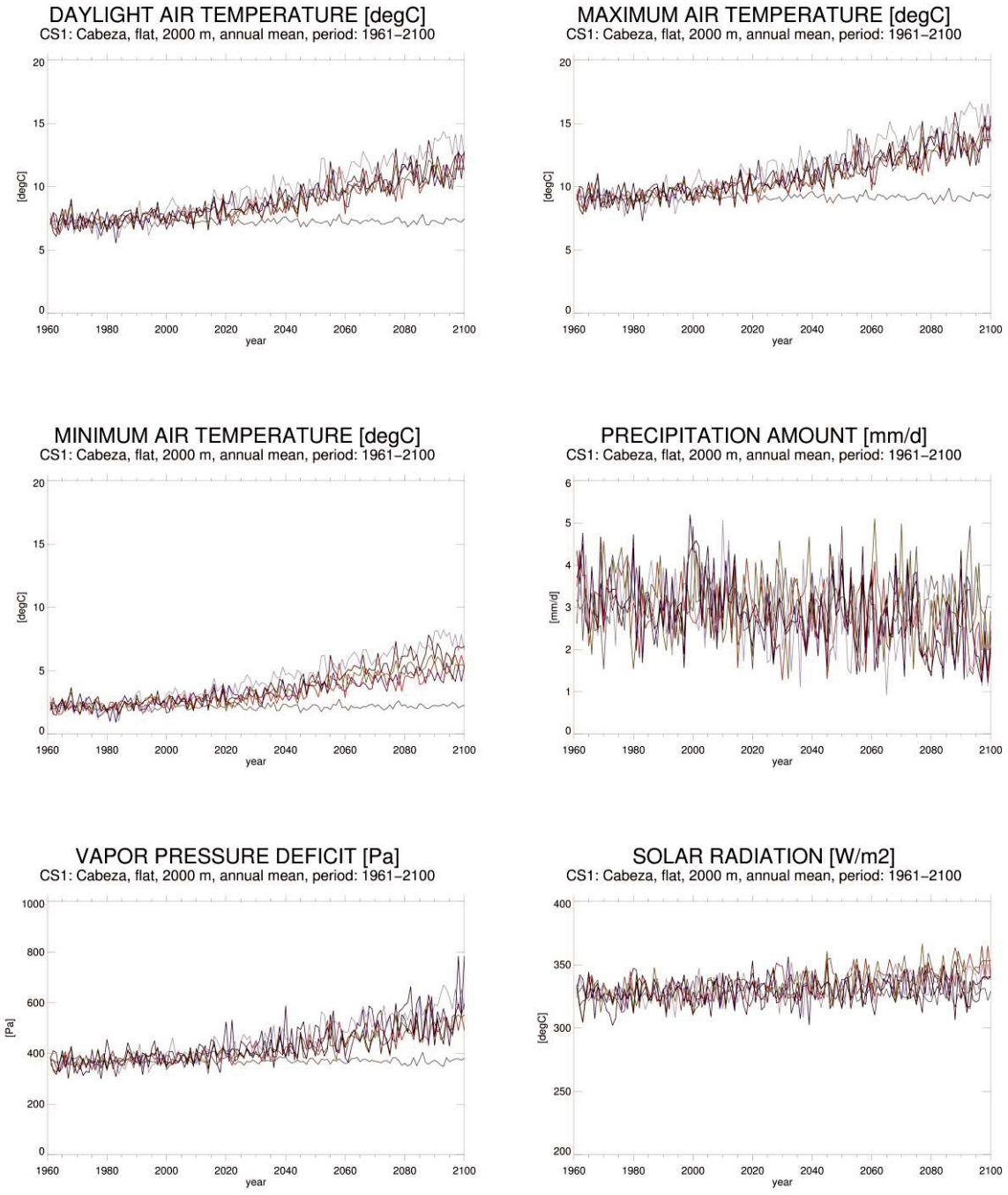

Figure 6: Effect of climate change in CS1, Cabeza de Hierro, expressed in terms of the evolution of annual mean values of daylight, minimum, and maximum temperature, precipitation, vapour pressure deficit, and global radiation (all bias corrected) from 1961 to 2100. The graphs depict the selected representative five simulations (cf. Table 2; coloured lines) and the baseline climate (black line).

Literature

Déqué, M. and S. Somot (2010), Weighted frequency distributions express modelling uncertainties in the ENSEMBLES regional climate experiments, *Clim. Res., 44*, 195–209, doi: 10.3354/cr00866

Déqué, M., D.P. Rowell, D. Lüthi, F. Giorgi, J.H. Christensen, B. Rockel, D. Jacob, E. Kjellström, M. de Castro and B. van den Hurk (2007), An intercomparison of regional climate simulations for Europe: assessing uncertainties in model projections, *Clim. Change, 81*, 53-70, doi:10.1007/s10584-006-9228-x.

Dettinger, M. D., D. R. Cayan, M. K. Meyer, A. E. Jeton (2004), Simulated hydrologic responses to climate variations and change in the Merced, Carson, and American river basins, Sierra Nevada, California, 1900-2099, *Climatic Change, 62*, 283-317.

Dobler, A. and B. Ahrens (2008), Precipitation by a regional climate model and bias correction in Europe and South Asia, *Meteorolog. Z., 17*, 499-509.

Finger, D., G. Heinrich, A. Gobiet, A. Bauder (2012), Assessing future water resources and its uncertainty in a glaciated alpine catchment and its subsequent effects on hydropower operations during the 21st century, *Water Resources Research, 48*, 20 pp, doi:10.1029/2011WR010733.

Frei, C., J. H. Christensen, M. Déqué, D. Jacob, R. G. Jones, P. L. Vidale (2003), Daily precipitation statistics in regional climate models: Evaluation and intercomparison for the European Alps, *Journal of Geophysical Research, 108* (D3), 4124, doi: 10.1029/2002JD002287.

Giorgi, F. And E. Coppola E (2007), European climate-change oscillation (ECO), *Geophys. Res. Lett., 34*, L21703, doi:10.1029/2007GL031223

Gutowski, W. J. Jr., S. G. Decker, R. A. Donavon, Z. Pan, R. W. Arritt, E. S. Takle (2003), Temporal Spatial Scales of Observed and Simulated Precipitation in Central U.S. Climate. *J. of Climate, 16*, 3841–3847, doi:10.1175/1520-0442(2003) 016 3841:TSOOAS 2.0.CO;2.

Hagemann, S., B. Machenhauer, R. Jones, O. B. Christensen, M. Déqué, D. Jacob, P. L. Vidale (2004), Evaluation of Water and Energy Budgets in Regional Climate Models Applied Over Europe, *Climate Dynamics, 23*, 547-567.

Haylock, M. R., N. Hofstra, A. M. G. Klein-Tank, E. J. Klok, P. D. Jones, M. New (2008), A European daily high-resolution gridded dataset of surface temperature and precipitation, *JGR (Atmospheres), 113*, 1–12, D20119, doi:10.1029/2008JD10201.

Heinrich, G., A. Gobiet, T. Mendlik (2013), Extended regional climate model projections for Europe until the mid-21st century: combining ENSEMBLES and CMIP3, *Clim. Dyn.,* published "online first", doi: 10.1007/s00382-013-1840-7

Hewitt, C. D. and D. J. Griggs (2004), Ensembles-Based Predictions of Climate Changes and Their Impacts (ENSEMBLES), *Eos Trans. AGU, 85*(52), 566, doi: 10.1029/2004EO520005.

Knutti, R., R. Furrer, C. Tebaldi, J. Cermak, G. A. Meehl GA (2010), Challenges in combining projections from multiple climate models, *J. Climate, 23*, 2739–2758, doi: 10.1175/2009JCLI3361.1

Maraun D., A. Ireson, F. Wetterhall, S. Bachner, E. Kendon, H. W. Rust, V. K. C. Venema, M. Widmann, R. E. Chandler, C. J. Onof, T. J. Osborn, T. Sautner, M. Themeßl, I. Thiele-Eich (2010), Statistical downscaling and modelling of precipitation. Bridging the gab between dynamical models and the end users. *Reviews of Geophysics, 48*(3), 1–34.

Mendlik, T., R.A.I. Wilcke, A. Gobiet, G. Heinrich (2012), *ACQWA Deliverable S.2.6: Performance and uncertainty in fine scale downscaling techniques*, WEGC Report to EU-FP7 212250, 15 pp., Wegener Center, University of Graz, Graz, Austria, available via www.uni-graz.at/igam7www_mendlik_etal-2012-acqwa-deliverable_26.pdf (28.6.2013).

Nakicenovic N., J. Alcamo, G. Davis, B. de Vries, J. Fenhann, S. Gaffin, K. Gregory, A. Grübler, T. Y. Jung, T. Kram, E. L. La Rovere, L. Michaelis, S. Mori, T. Morita, W. Pepper, H. Pitcher, L. Price, K. Raihi, A. Roehrl, H.-H. Rogner, A. Sankovski, M. Schlesinger, P. Shukla, S. Smith, R. Swart, S. van Rooijen, N. Victor, Z. Dadi (2000), *IPCC Special Report on Emissions Scenarios*. Cambridge University Press: Cambridge, United Kingdom, and New York.

Panofsky H. W., G. W. Brier (1968), *Some Applications of Statistics to Meteorology*. The Pennsylvania State University Press: Philadelphia.

Piani, C., J. O. Haerter, and E. Coppola (2010), Statistical bias correction for daily precipitation in regional climate models over Europe, *Theoretical and Applied Climatology, 99*(1-2), 187-192, doi: 10.1007/s00704-009-0134-9.

Racsko, P., Szeidl, L. and Semenov, M., 1991. A serial approach to local stochastic weather models. *Ecological Modelling, 57*(1–2), 27-41.

Running, S.W., R.R. Nemani, and R.D. Hungerford (1987), Extrapolation of synoptic meteorological data in mountainous terrain and its use for simulating forest evapotranspiration and photosynthesis, *Canadian Journal of Forest Research, 17*, 472-483.

Semenov, M.A. and E.M. Barrow (1997), Use of a stochastic weather generator in the development of climate change scenarios, *Climatic Change, 35*(4), 397-414.

Stainforth, D. A., M. R. Allen, E. R. Tredger, L. A. Smith (2007), Confidence, uncertainty and decision-support relevance in climate predictions, *Phil. Trans. R. Soc. A*, *365*, 2145-2161, doi: 10.1098/rsta.2007.2074

Suklitsch, M., A. Gobiet, A. Leuprecht, C. Frei (2008), High Resolution Sensitivity Studies with the Regional Climate Model CCLM in the Alpine Region, *Meteorologische Zeitschrift, 17*(4), 467-476.

Suklitsch, M., A. Gobiet, H. Truhetz, N. K. Awan, H. Göttel, and D. Jacob (2011), Error Characteristics of High Resolution Regional Climate Models over the Alpine Area, *Clim. Dyn., 37* (1-2), 377–390, doi: 10.1007/s00382-010-0848-5.

Themeßl, M. J., A. Gobiet, and A. Leuprecht (2011), Empirical-statistical downscaling and error correction of daily precipitation from regional climate models, *Int. J. Climatol., 31*(10), 1530–1544, doi: 10.1002/joc.2168.

Themeßl, M. J., A. Gobiet, and G. Heinrich (2012), Empirical-statistical downscaling and error correction of daily precipitation of regional climate models and its impact on the climate change signal, *Clim. Change, 112*(2), 449-468, doi: 10.1007/s10584-011-0224-4.

Thornton, P.E. and S. W. Running (1999), An improved algorithm for estimating incident daily solar radiation from measurements of temperature, humidity, and precipitation. Agricultural and Forest Meteorology, 93(4): 211-228.

Thurnher, C. (2013), *Component of ARANGE Deliverable D1.1 – Baseline Climate*, ARANGE Internal Report, 10 pp, Institute for Silviculture and Forest Engeneering, University of Life Sciences Vienna, Vienna, Austria.

Wilcke, R.A.I., T. Mendlik, A. Gobiet (2013), Multi-Variable Error Correction of Regional Climate Models, Climatic Change, minor revisions.

Wood, A. W., L. R. Leung, V. Sridhar, D. P. Lettenmaier (2004), Hydrologic Implications of Dynamical and Statistical Approaches to Downscale Climate Model Outputs, *Clim. Change, 62*, 189-216.

Appendix – Climate Change Signals

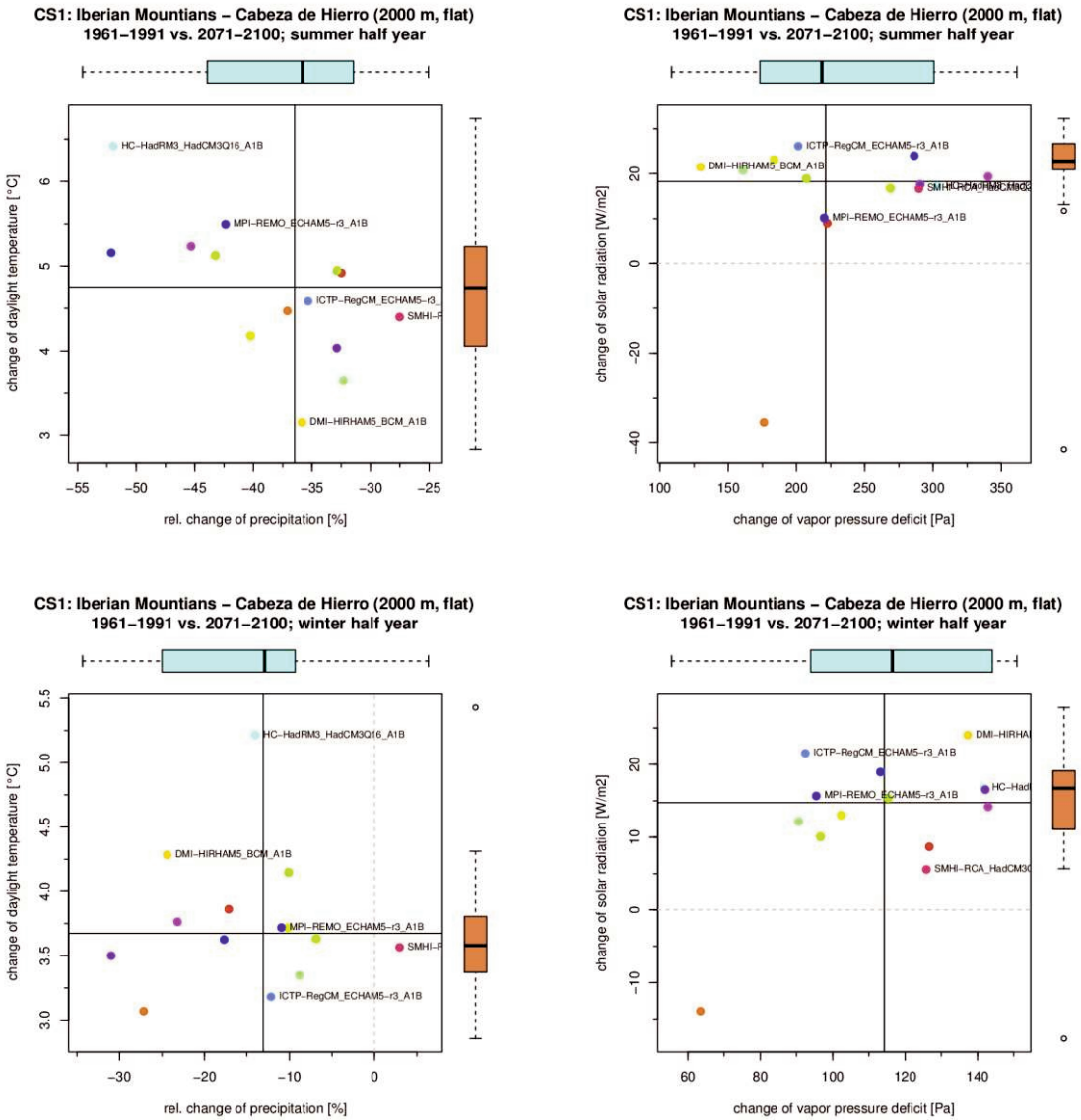

Figure A-1: Climate change signals of daylight temperature [°C], precipitation [%], solar radiation [W/m^2], and vapor pressure deficit [Pa] in case study region CS1, Cabeza de Hierro, on a flat plane elevated to 2000 m. Differences between the periods 1961 to 1990 and 2071 to 2100 of half year means (summer half year: upper row; winter half year: lower row) from downscaled and corrected ENSEMBLES simulations are shown. Selected representative simulations are labeled.

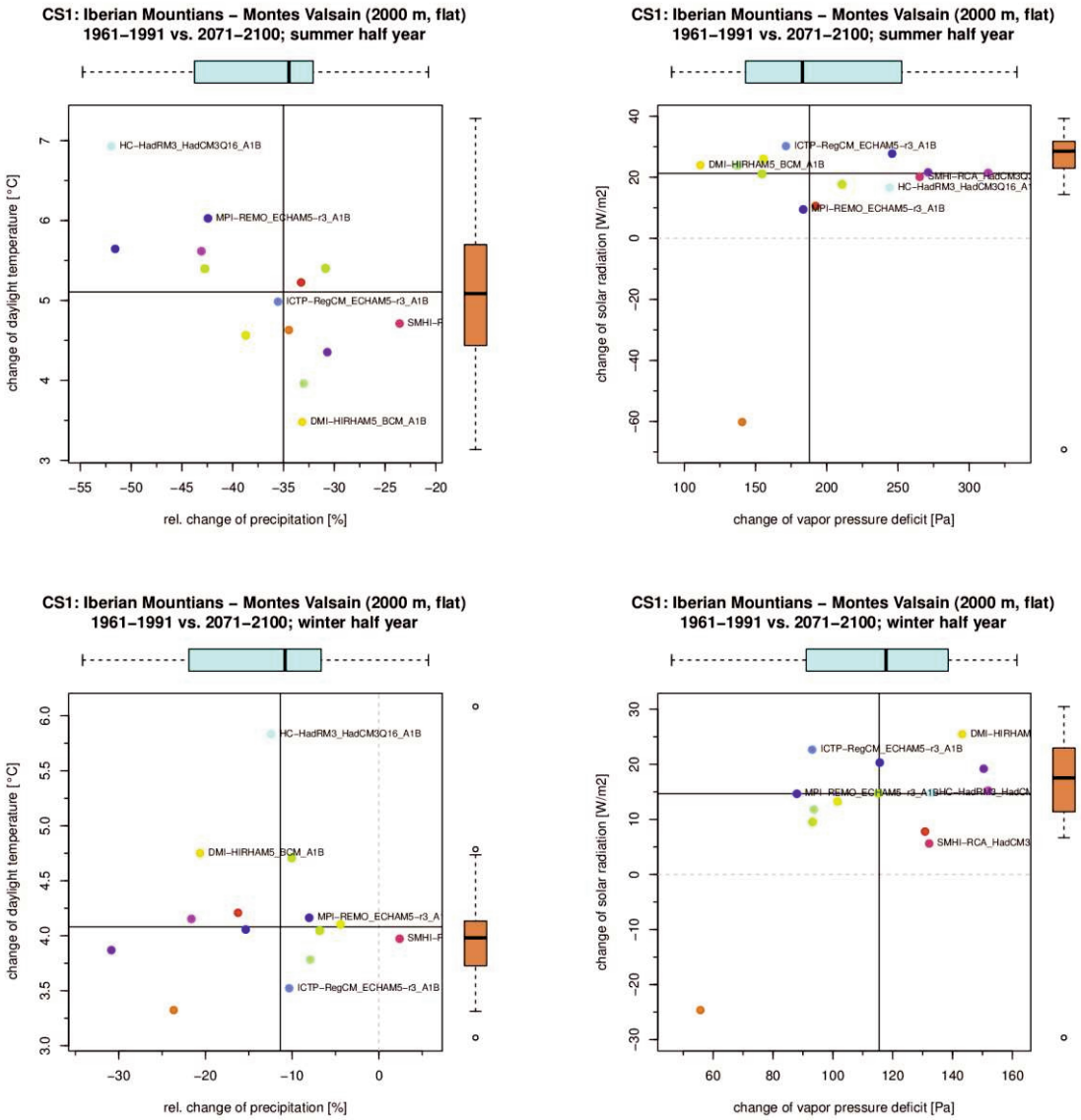

Figure A-2: Same as Figure , but for case study region CS1, Montes Valsain.

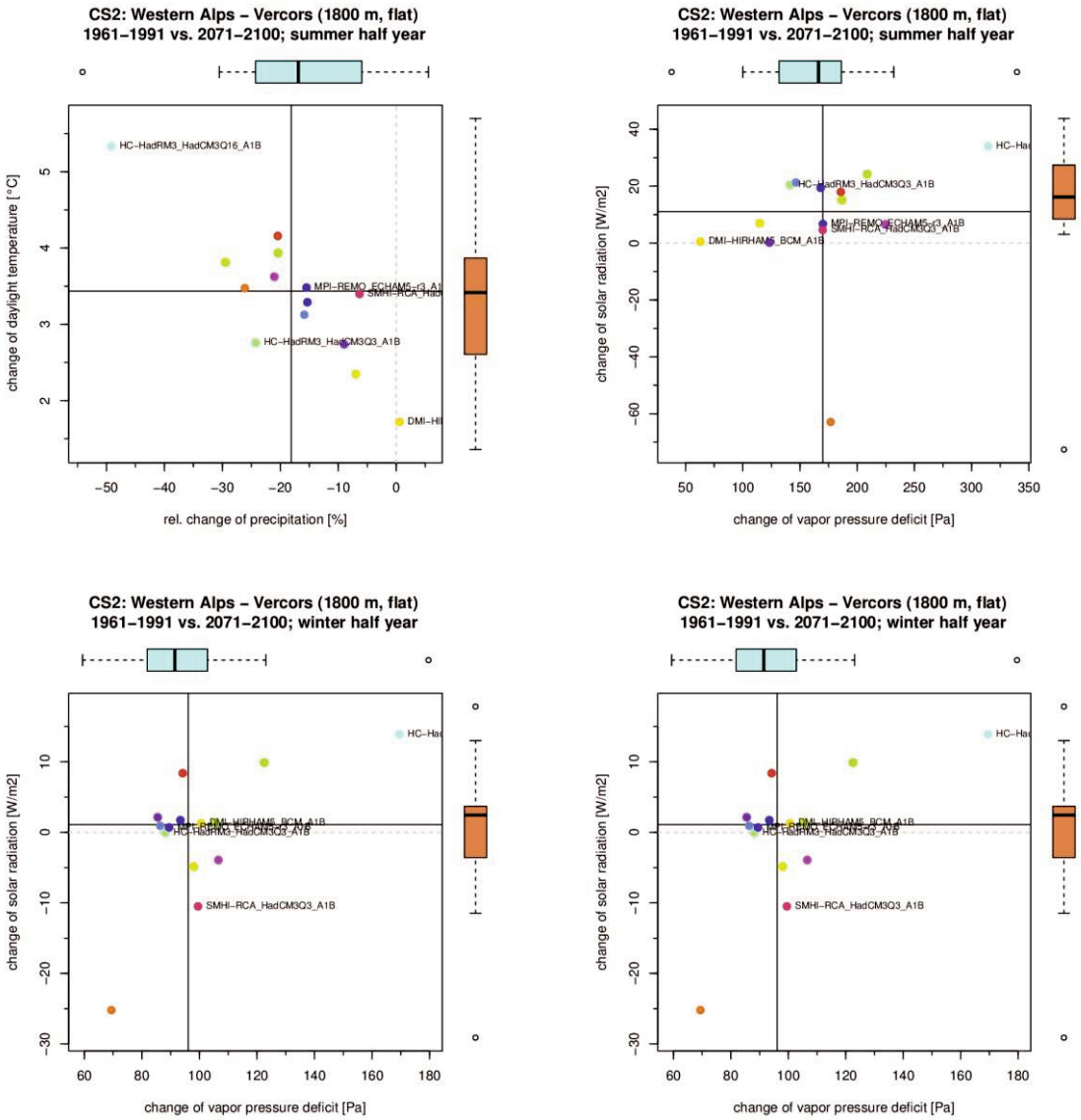

Figure A-3: Same as Figure , but for case study region CS2, Western Alps in 1800 m altitude.

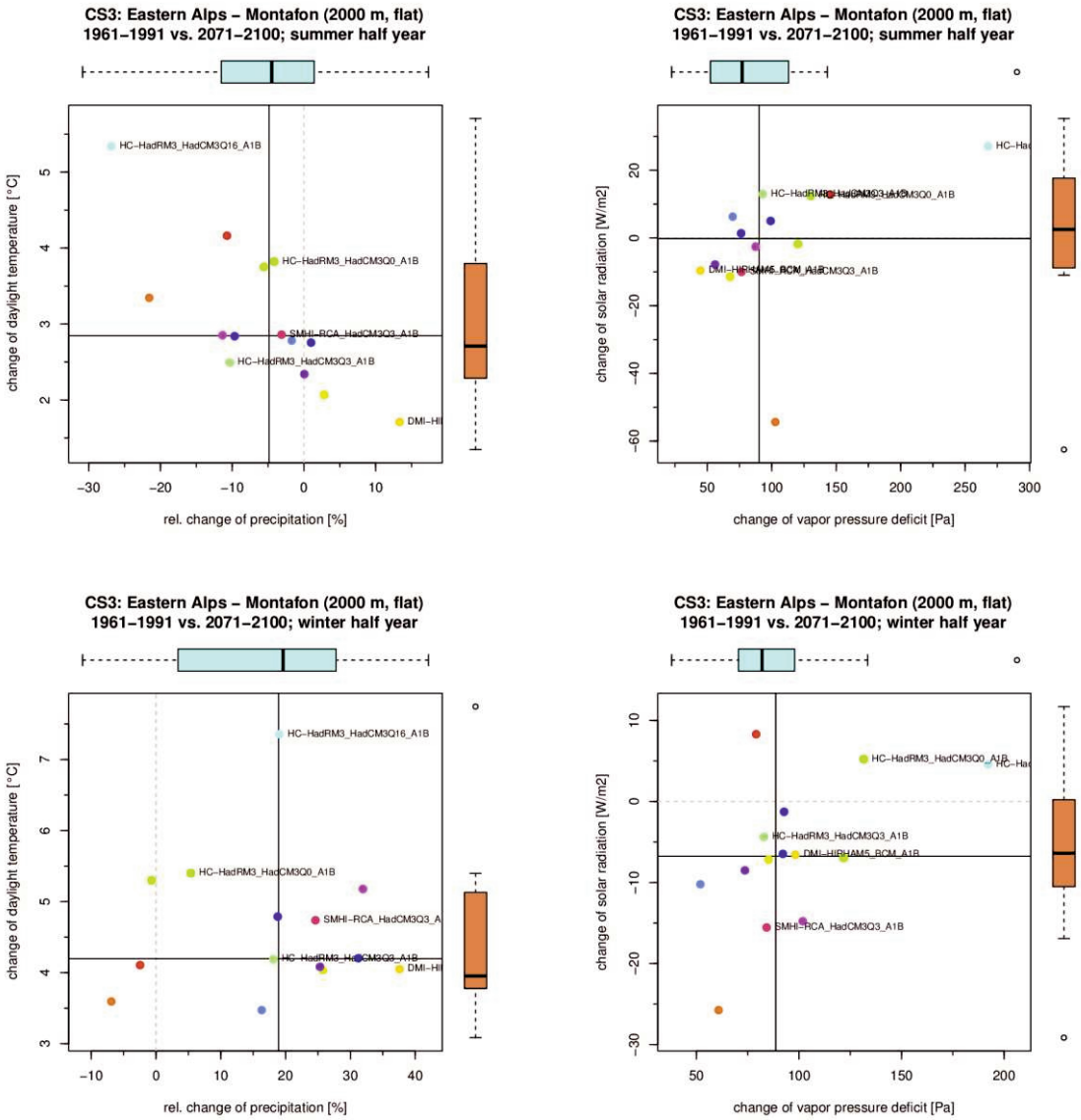

Figure A-4: Same as Figure , but for case study region CS3, Eastern Alps in 2000 m altitude.

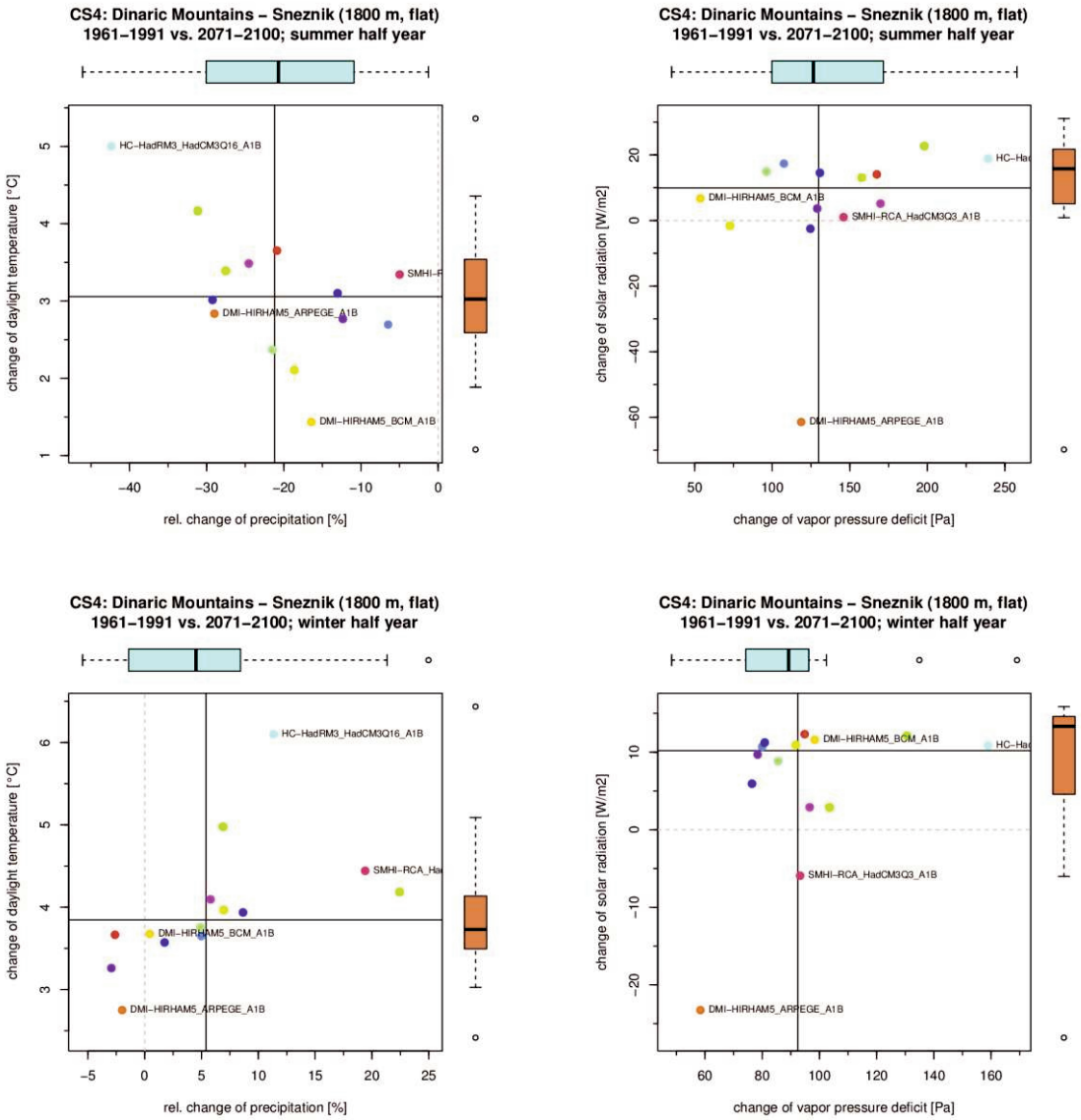

Figure A-5: Same as Figure , but for case study region CS4, Dinaric Mountains in 1800 m altitude.

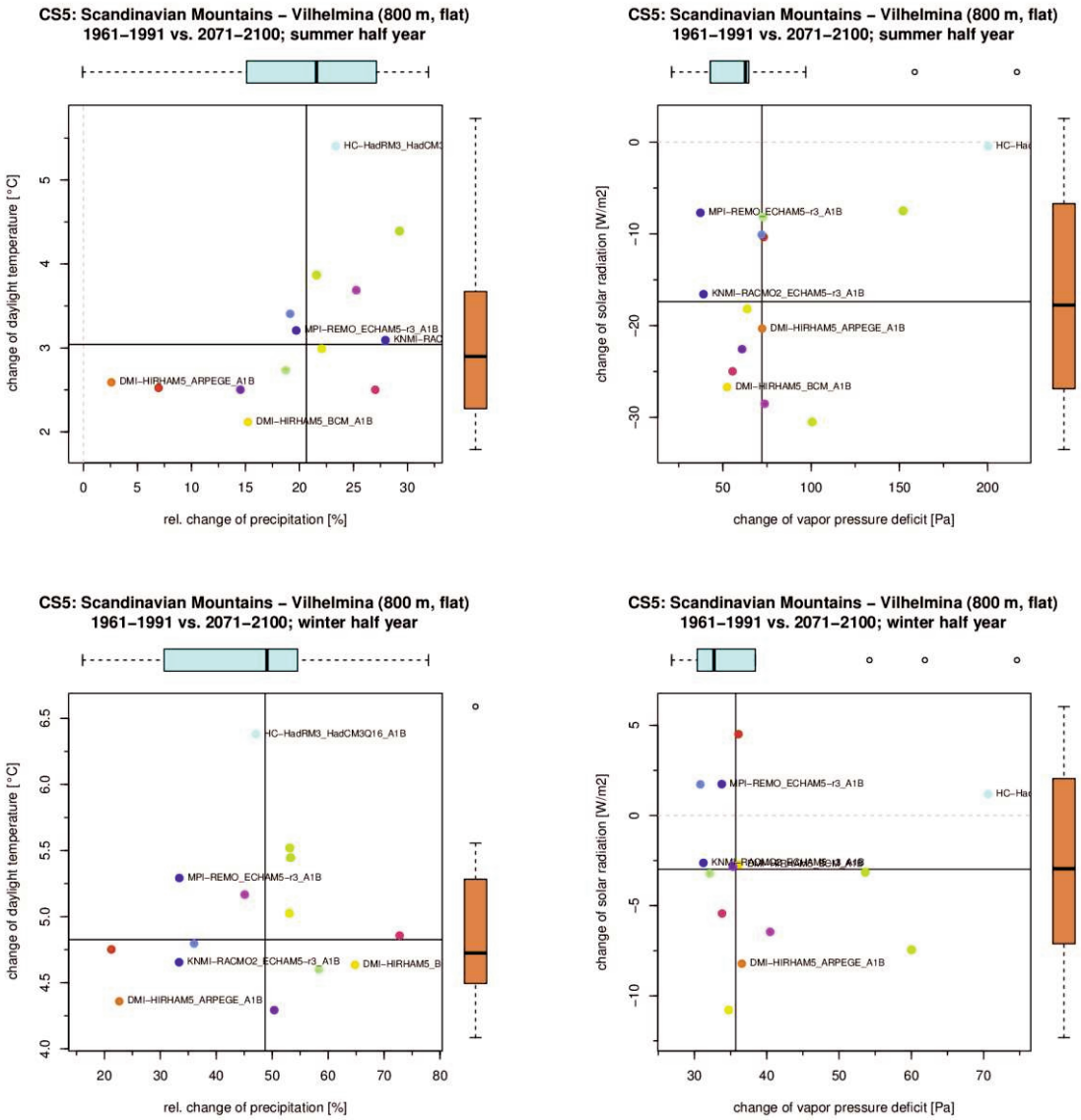

Figure A-6: Same as Figure , but for case study region CS5, Scandinavian Mountains in 800 m altitude.

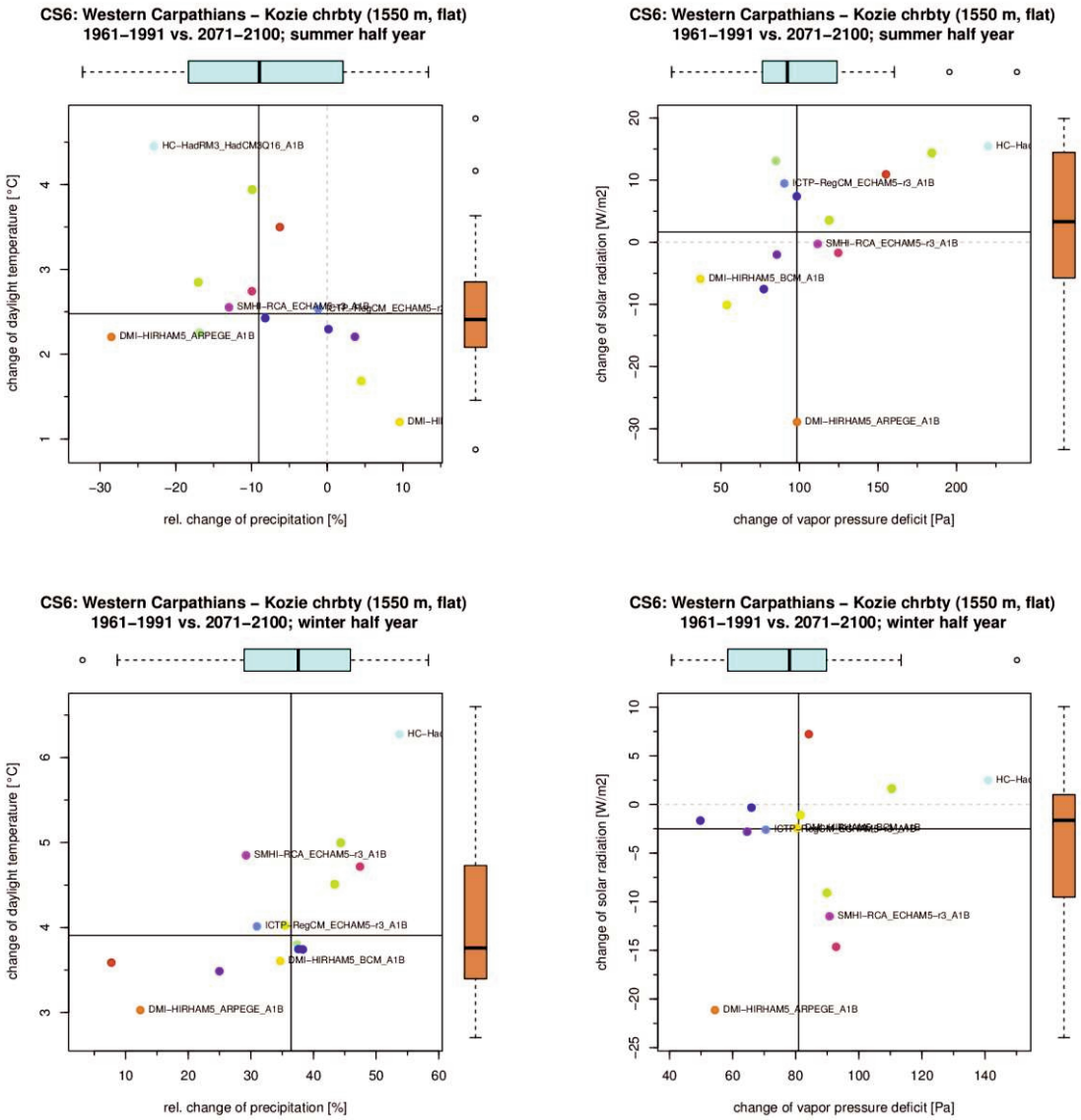

Figure A-7: Same as Figure , but for case study region CS6, Carpathians in 1550 m altitude.

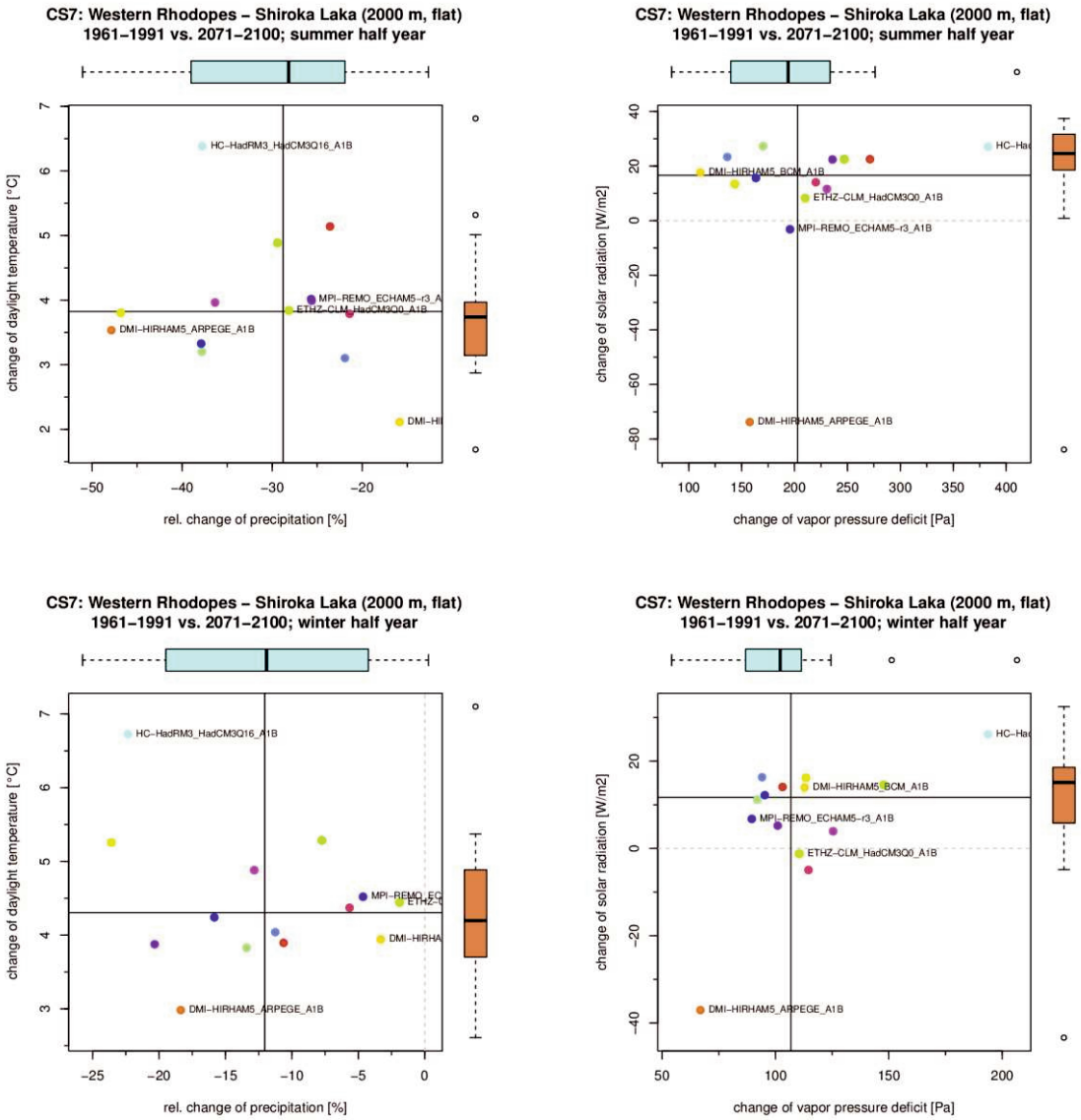

Figure A-8: Same as Figure , but for case study region CS7, Western Rhodopes in 2000 m altitude.